

# Ligand Exchange on Pyrazolate- $\kappa N$ - $\mu$ -pyrazolate and Pyrazole- $\kappa N$ - $\mu$ -pyrazolate Binuclear Nickel Complexes

Juan Cámpora, Jorge A. López, Celia M. Maya, Pilar Palma,\* and Ernesto Carmona

Departamento de Química Inorgánica, Instituto de Investigaciones Químicas, Universidad de Sevilla, Consejo Superior de Investigaciones Científicas, C/Americo Vespucio s/n, Isla de la Cartuja, 41092 Sevilla, Spain

Caridad Ruíz

Instituto de Ciencia de Materiales de Madrid, Consejo Superior de Investigaciones Científicas, Campus de Cantoblanco, 28049 Madrid, Spain

Received January 19, 2000

Compounds containing bridging pyrazolate and terminal pyrazolate or pyrazole ligands of type  $\text{Ni}_2(\text{PMe}_3)_2(\text{L}-\kappa N)(\mu_2-\eta^1:\eta^3-\text{CH}_2-o\text{-C}_6\text{H}_4)(\mu_2-\text{L}-\kappa N, N)$  ( $\text{L} = 3,5$ -dimethylpyrazolate ( $\text{Pz}'$ ), **3b**, or 3,5-di-*tert*-butylpyrazolate ( $\text{Pz}^{**}$ ), **3c**);  $\text{Ni}_2(\text{PMe}_3)_2(\text{Pz}^{**}-\kappa N)(\mu_2-\eta^1:\eta^3-\text{CH}_2-o\text{-C}_6\text{H}_4)(\mu_2-\text{Pz}'-\kappa N, N)$ , **4**, and  $[\text{Ni}_2(\text{PMe}_3)_2(\text{HPz}''-\kappa N)(\mu_2-\eta^1:\eta^3-\text{CH}_2-o\text{-C}_6\text{H}_4)(\mu_2-\text{Pz}-\kappa NN)](\text{X})$  ( $\text{X} = \text{Br}$ , **5**, or  $\text{BPh}_4$ , **6**) have been prepared. Spin saturation transfer experiments reveal a slow motion of the terminal pyrazolate ligand of **3b** and **4**, consisting of a combination of N,N-metallotropic shift and rotation around the Ni–N bond, but did not show any exchange of the bridging and terminal pyrazolate ligands. However, the mixed ligand derivative **4** can be obtained by conproportionation of **3b** and **3c**. This reaction reveals a slow intermolecular bridging–terminal as well as intermolecular pyrazolate exchange. In contrast with complexes of type **3** and **4**, the formally cationic **5** and **6** display dynamic NMR spectra at room temperature due to their occurrence in solution as a mixture of rapidly exchanging isomers. Variable-temperature NMR experiments have shown that **5** also undergoes a highly stereoselective  $\text{HPz}/\text{Br}^-$  exchange.

## Introduction

Pyrazoles (HPz) and pyrazolate ( $\text{Pz}^-$ ) anions are attractive ligands that exhibit a very rich coordination chemistry.<sup>1</sup> Usually pyrazole and substituted pyrazoles behave as monodentate ligands,<sup>2</sup> examples of monodentate pyrazolates being comparatively less common,<sup>3</sup> because of their pronounced tendency to bridge two metal centers.<sup>4</sup> Monodentate pyrazole or pyrazolate ligands may give rise to interesting processes such as prototropic equilibria or reversible metal–ligand binding, which are relevant to biological systems.<sup>5</sup>

We have described recently several binuclear complexes of nickel that contain bridging hydrocarbyl and pyrazolate ligands (e.g., compounds **1a–c** of Scheme 1).<sup>6</sup>

(1) (a) Trofimenko, S. *Prog. Inorg. Chem.* **1986**, *34*, 115. (b) Steel, J. P. *Coord. Chem. Rev.* **1990**, *106*, 227. (c) Cosgriff, J. E.; Deacon, G. B. *Angew. Chem., Int. Ed.* **1998**, *37*, 286. (d) Deacon, G. B.; Delbridge, E. E.; Skelton, B. W.; White, A. H. *Angew. Chem., Int. Ed.* **1998**, *37*, 2251.

(2) (a) López, G.; Ruiz, J.; Vicent, C.; Martí, J. M.; García, G.; Chaloner, P. A.; Hitchcock, P. B.; Harrison, R. M. *Organometallics* **1992**, *11*, 4090. (b) Esteruelas, M. A.; Lahoz, F. J.; Oro, L. A.; Oñate, E.; Ruiz, N. *Inorg. Chem.* **1994**, *33*, 787. (c) García, M. P.; Esteruelas, M. A.; Martín, M.; Oro, L. A. *J. Organomet. Chem.* **1994**, *467*, 151. (d) Cano, M.; Campo, J. A.; Heras, J. V.; Lafuente, J.; Rivas, C.; Pinilla, E. *Polyhedron* **1995**, *14*, 1139.

(3) For some recent examples, see: (a) Carmona, D.; Lahoz, F. J.; Oro, L. A.; Lamata, M. P.; Buzarra, S. *Organometallics* **1991**, *10*, 3123. (b) Lezdings, P.; Rettig, S. J.; Smith, K. H.; Tong, V. *J. Chem. Soc., Dalton Trans.* **1997**, 3269. (c) Au, S. M.; Fung, W. H.; Chang, M.; Che, C. M.; Peng, S. M. *J. Chem. Soc., Chem. Commun.* **1997**, 182. (d) Guzei, I. A.; Yap, G. P. A.; Winter, C. H. *Inorg. Chem.* **1997**, *36*, 1738.

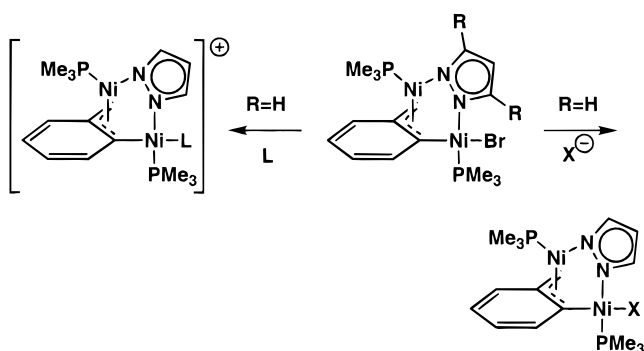
The pyrazolate unit of these complexes undergoes a slow dynamic process that exchanges the relative positions of its 3 and 5 substituents. In turn, the coordinated bromide is labile, and it can be displaced readily by some formally anionic (e.g., 2,5-dimethylpyrrolyl) or neutral ( $\text{PMe}_3$ ,  $\text{Me}_2\text{PCH}_2\text{CH}_2\text{PMe}_2$ ) ligands. In view of these findings, we have considered worthwhile their extension by replacing the  $\text{Br}^-$  group by a second pyrazolate fragment or by a molecule of the neutral pyrazole. The new compounds contain two potentially bridging pyrazole-type ligands. However, since no other chemical or

(4) (a) Coleman, A. W.; Eadie, D. T.; Stobart, S. R.; Zaworotko, M. J.; Atwood, J. L. *J. Am. Chem. Soc.* **1982**, *104*, 922. (b) Marshall, J. L.; Hopkins, M. D.; Miskowski, V. M.; Gray, H. B. *Inorg. Chem.* **1992**, *31*, 5034. (c) López, G.; Ruiz, J.; García, G.; Vicente, C.; Casabó, J.; Molins, E.; Miravittles, C. *Inorg. Chem.* **1991**, *30*, 2605. (d) Jain, V. K.; Kannan, S.; Tienkink, E. R. T. *J. Chem. Soc., Dalton Trans.* **1993**, 3625. (e) Carmona, D.; Mendoza, A.; Ferrer, J.; Lahoz, F. J.; Oro, L. A. *J. Organomet. Chem.* **1992**, *431*, 87. (f) López, G.; Ruiz, J.; García, G.; Vicente, C.; Rodríguez, V.; Sánchez, G.; Hermoso, J. A.; Martínez-Ripoll, M. *J. Chem. Soc., Dalton Trans.* **1992**, 1681. (g) López, G.; García, G.; Sánchez, G.; García, J.; Vegas, A.; Martínez-Ripoll, M. *Inorg. Chem.* **1992**, *31*, 1518. (h) Carmona, D.; Lamata, P. M.; Esteban, M.; Lahoz, F. J.; Oro, L. A.; Apreada, M. C.; Foces-Foces, C.; Cano, F. H. *J. Chem. Soc., Dalton Trans.* **1994**, 159. (i) Carmona, D.; Ferrer, J.; Mendoza, A.; Lahoz, F.; Reyes, J.; Oro, L. A. *Angew. Chem., Int. Ed. Engl.* **1991**, *30*, 1171. (j) Beveridge, K. A.; Bushnell, G. W.; Stobart, S. R.; Atwood, J. L.; Zaworotko, M. J. *Organometallics* **1983**, *2*, 1447.

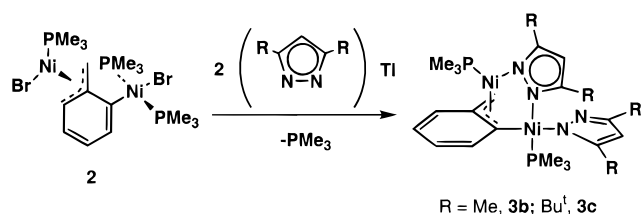
(5) (a) Cowan, J. A. *Inorganic Biochemistry, An Introduction*; VCH: New York, 1993. (b) Kitajama, N.; Tolman, W. *Prog. Inorg. Chem.* **1995**, *43*, 419. (c) Govind, B.; Satyanarayana, T.; Veera-Reddy, K. *Polyhedron* **1995**, *15*, 1009, and references therein.

(6) Cámpora, J.; López, J. A.; Palma, P.; Ruiz, C.; Carmona, E. *Organometallics* **1997**, *16*, 2709.

Scheme 1



Scheme 2

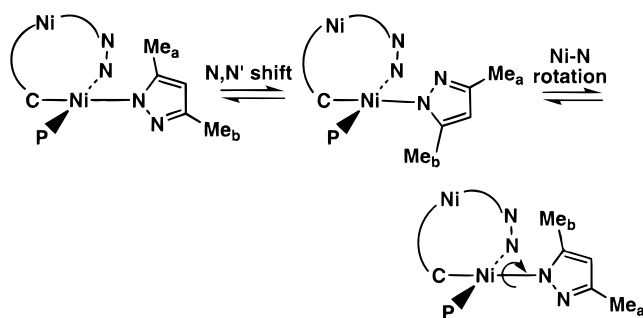


structural changes accompany this substitution reaction, only one of them can actually join the two metal centers. Complexes that have simultaneously bridging and terminal pyrazolate ligands while uncommon<sup>7</sup> are amenable to mechanistic studies aimed at ascertaining the possibility of exchange between the two Pz units. Here we discuss in detail the results of our investigation of this problem.

## Results and Discussion

**Compounds Containing Bridging and Terminal Pyrazolate Ligands.** Rather unexpectedly, the reaction of **1a** with equimolar quantities of LiPz fails to give the bis(pyrazolate) derivative **3a** (vide infra). Analogous complexes of the 3,5-dimethylpyrazolate (Pz'') (**3b**) and 3,5-di-*tert*-butylpyrazolate (Pz'') (**3c**) ligands can however be obtained in ca. 90 and 35% yield, respectively, by the reaction (Scheme 2) of the binuclear nickel complex<sup>8</sup> **2** with 2 molar equiv of the appropriate thallium pyrazolate salt.<sup>9</sup> The NMR spectra of **3b** and **3c** are similar to those of complexes **1a–c**<sup>6</sup> and are therefore in accord with the presence of a bridging pyrazolate ligand and a  $\mu^2\text{-}\eta^3\text{:}\eta^1\text{-C}_7\text{H}_6$  fragment that coordinates in such a manner as to allow the maximum proximity of the two nickel centers. Each pyrazolate ligand gives rise to an independent set of signals, their two Me or Bu<sup>t</sup> substituents being in addition inequivalent (see Experimental Section). The precise assignment of those corresponding to the bridging and terminal ligands cannot be made on the basis of these spectra. Even though **3b** and **3c** are susceptible to undergoing

Scheme 3



intramolecular bridging-terminal ligand exchange, the NMR spectra display sharp signals at room temperature for the two pyrazolate units, indicating that if such an exchange takes place, it is too slow to cause any line broadening. However spin saturation transfer experiments provide interesting information, saturation of the methyl signal of **3b** at  $\delta$  2.84 ppm resulting in a very efficient magnetization transfer to other higher-field Me signal at  $\delta$  2.19 ppm (ca. 80%). The rate for the methyl group exchange, quantitatively determined from a standard magnetization transfer experiment,<sup>10b</sup> is  $2.02(11) \text{ s}^{-1}$  at 20 °C. Although the proximity of the other two Me signals ( $\delta$  1.71 and 1.64 ppm) makes difficult a reliable measurement, the saturation of any of these does not result in an appreciable (<5%) magnetization transfer to any other signal. These observations are in disagreement with a bridging-terminal pyrazolate exchange and reveal instead the existence of a dynamic process that involves only one of these fragments. Since the rotation of the bridging pyrazolate ligand in the parent compounds **1** is at least 3 orders of magnitude slower,<sup>6</sup> it appears reasonable to propose that the above exchange involves the terminal pyrazolate unit. The Me-group interconversion could be effected by an N,N-metallotropic shift, combined with a rotation around the Ni–N bond, as shown in Scheme 3. Since the N,N metal shift is expected to be a facile process,<sup>11</sup> it is very possible that the energy barrier associated with the interchange is due to hindered rotation caused by the pyrazolate substituents. In accord with this assumption no exchange of this type has been detected for the Bu<sup>t</sup> derivative **3c** at room temperature.

A mixed pyrazolate-ligand complex **4** has also been obtained, and whereas two isomeric structures may be proposed for this compound, only that containing bridging Pz'' and terminal Pz''\* has been generated. This is regardless of the nature of the compound (**1b** or **1c**) used as the starting material (Scheme 4). The ligand arrangement of **4** seems to be more favorable on steric grounds than that of the isomeric structure **4'**; since it could not be unequivocally ascertained from the avail-

(7) (a) Oro, L. A.; Carmona, D.; Lamata, M. P.; Foces-Foces, C.; Cano, F. M. *Inorg. Chim. Acta* **1985**, *97*, 19. (b) Carmona, D.; Oro, L. A.; Lamata, H. P.; Jimeno, M. L.; Elguero, J.; Belguise, A.; Lux, P. *Inorg. Chem.* **1994**, *33*, 2196. (c) Carmona, D.; Ferrer, J.; Atencio, R.; Lahoz, F. J.; Oro, L. A.; Lamata, M. P. *Organometallics* **1995**, *14*, 2057.

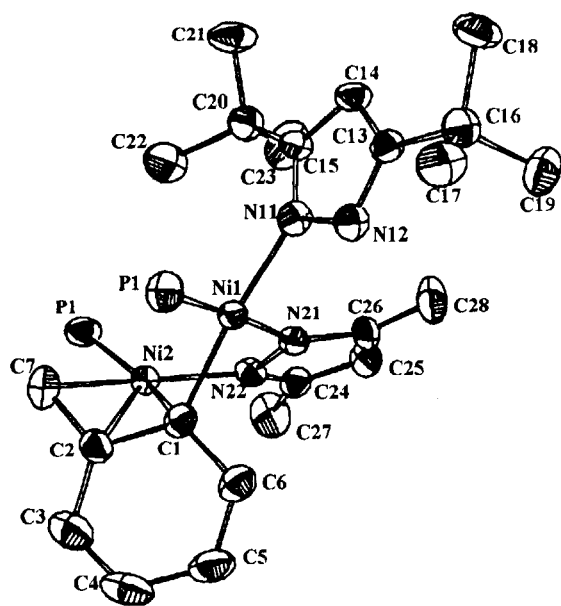
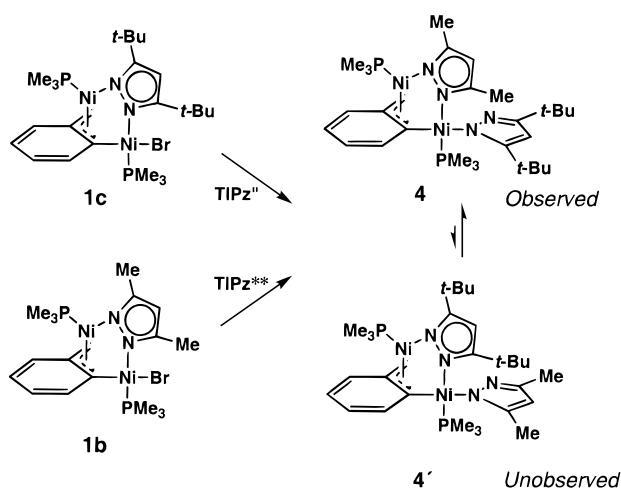
(8) Cámpora, J.; Gutiérrez, E.; Monge, A.; Poveda, M. L.; Carmona, E. *Organometallics* **1992**, *11*, 2644.

(9) Deacon, G. B.; Delbridge, E. E.; Forsyth, C. M.; Skelton, B. W.; White, A. J. *J. Chem. Soc., Dalton Trans.* **2000**, 745.

(10) (a) Sandström, J. *Dynamic NMR Spectroscopy*; Academic Press: New York, 1982. (b) Green, M. L. H.; Sella, A.; Wong, L. L. *Organometallics* **1992**, *11*, 2650. (c) Supposing that  $T_1$  values are similar for all methyl substituents on pyrazole rings, the exchange rate between two of these groups is inversely proportional to the decrease of the intensity of one of their signals after the saturation of the other Me group signal. Houser, E. J.; Venturelli, A.; Rauchfuss, T. B.; Wilson, S. R. *Inorg. Chem.* **1995**, *34*, 6602.

(11) (a) Abel, E. W.; Heard, P. J.; Orrell, K. G.; Sik, V. *Polyhedron* **1994**, *13*, 2907. (b) Alvarez, S.; Bermejo, M. J.; Vinaixa, J. *J. Am. Chem. Soc.* **1987**, *109*, 5136. (c) Kang, S. K.; Albright, T. A.; Mealli, C. *Inorg. Chem.* **1987**, *26*, 3158. (d) Jackson, W. G.; Cortez, S. *Inorg. Chem.* **1994**, *33*, 1921.

Scheme 4

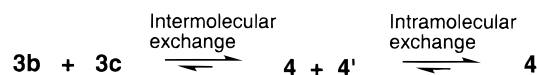
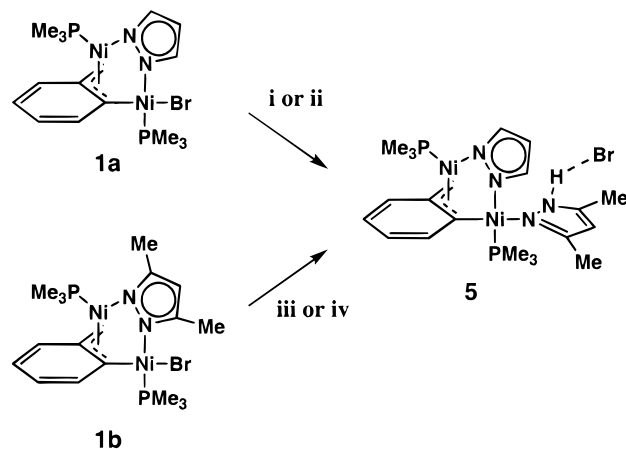


**Figure 1.** ORTEP view and atom-labeling scheme of compound **4**. The methyl groups of PMe<sub>3</sub> ligands have been omitted.

able NMR data, confirmation by a single-crystal X-ray study (to be discussed later) proved necessary.

As observed for **3b**, saturation of the <sup>1</sup>H signals corresponding to the Bu<sup>t</sup> substituents of the Pz\*\* ligand of **4** reveals their exchange. The rate of exchange is slow at room temperature, but the process becomes faster at 60 °C, ca. 40% magnetization transfer being detected at this temperature. In contrast, saturation of any of the bridging Pz'' methyl signals does not result in any appreciable decrease of the intensity of the other, even at the higher temperature. In accordance with the exchange mechanism proposed in Scheme 3, the energy barrier for the exchange process increases with the steric crowding of the molecule, resulting in the observed rate order **3b** < **4** < **3c**. Although it has not been possible to observe directly the bridging-to-terminal pyrazolate exchange for compound **4**, a consideration of Scheme 4 suggests that such conversion probably happens at some stage, at least during the reaction of **1c** with TIPz''. The question arises as to whether **4** is in equilibrium with the less-favored isomer **4'** or there is an irreversible rearrangement of **4'** to **4** under the

Scheme 5

Scheme 6<sup>a</sup>

<sup>a</sup> (i) LiPz'', THF, trace H<sub>2</sub>O; (ii) HPz''; (iii) LiPz, THF, trace H<sub>2</sub>O; (iv) HPz.

reaction conditions. To ascertain this point, we have prepared a solution containing equimolar amounts of **3b** and **3c** in CD<sub>2</sub>Cl<sub>2</sub> and monitored its evolution by <sup>31</sup>P{<sup>1</sup>H} NMR at room temperature. A clean conproportionation process could be observed, which led to **4** with *t*<sub>1/2</sub> ≈ 123 min. Small amounts (<10%) of three other minor species could be detected, two of them completely disappearing within 24 h. No further effort was done to ascertain the nature of these species, but since all of them displayed similar <sup>31</sup>P spin patterns (AB systems with *J*<sub>PP</sub> = 5–10 Hz), they are likely to correspond to structurally related molecules, such as **4'** or rotameric isomers of **3c**, **4**, or **4'**. This experiment also indicates that not only a slow intramolecular exchange of bridging and terminal pyrazolate ligands but also an intermolecular exchange of the terminal monodentate ligand take place in solution for compounds of type **3** and **4** (Scheme 5).

**Pyrazole-κN-μ-pyrazolate Complexes.** As briefly noted, we have unsuccessfully pursued the synthesis of complex **3a**, containing two unsubstituted Pz ligands. Similar attempts to obtain a mixed ligand compound of type **4**, having one bridging or terminal Pz ligand, have also proved fruitless. When compound **1a** is treated with 1 equiv of LiPz, only complex mixtures of uncharacterized products are formed. Moreover, low yields of compound **3b** are obtained if TIPz'' is used instead of LiPz. Despite the above, addition of 1 molar equiv of LiPz'' to **1a** proceeds as in Scheme 6 and gives rise to complex **5**, which contains a molecule of HPz coordinated to one of the Ni atoms. The same product is obtained if **1b** is reacted with LiPz.

The NMR spectra of compound **5** recorded in CD<sub>2</sub>Cl<sub>2</sub> at room temperature display broad signals, evidencing a fluxional behavior that will be discussed in detail below. It should be mentioned at this stage that the <sup>1</sup>H NMR spectrum exhibits two low-field broad signals at 14.1 and 15.0 ppm, with a relative intensity of ca. 1/2 H each. These are in the zone expected for N-bound pyrazole protons.<sup>12</sup> Clearly, the coordination of a neutral pyrazole ligand should result in the formation of a

Scheme 7

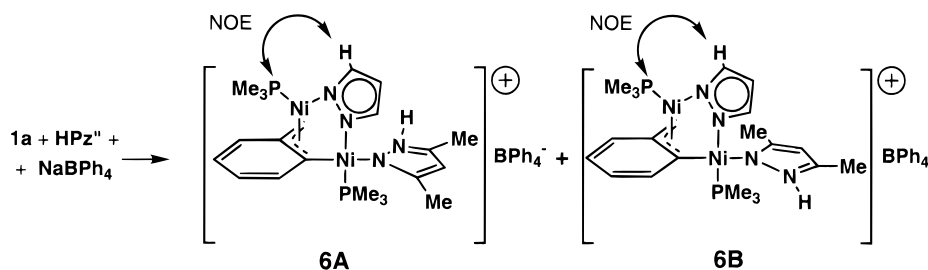
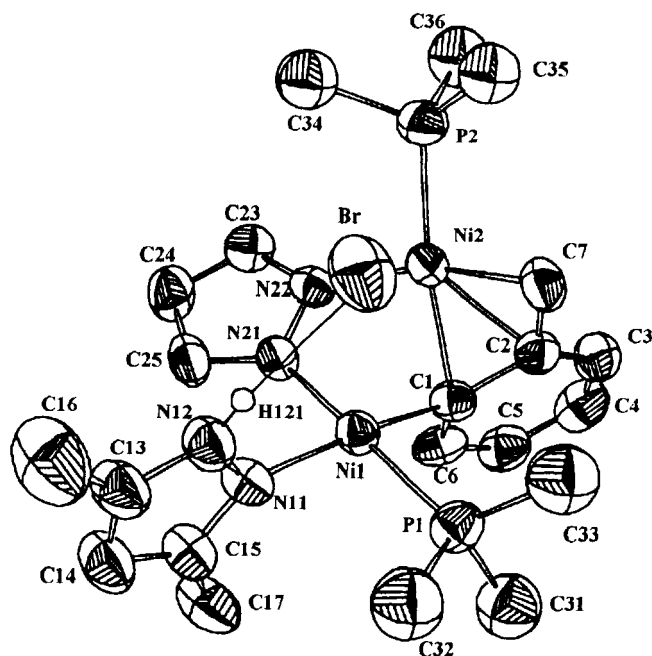
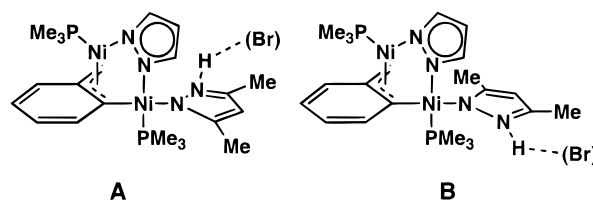


Chart 1



**Figure 2.** Crystal structure and atom-labeling scheme for compound **5**.

cationic species. Notwithstanding this, **5** is soluble in toluene and its solution in acetone shows low electrical conductivity ( $\Lambda_M(20\text{ }^\circ\text{C}) = 9.1\ \Omega^{-1}\ \text{cm}^2\ \text{mol}^{-1}$ ). In addition, no IR band could be clearly assigned to the IR  $\nu(\text{NH})$  stretching vibration. All these data suggest close association of the  $\text{Br}^-$  anion with the uncoordinated nitrogen of the molecule of pyrazole, by means of a  $\text{N}-\text{H}\cdots\text{Br}$  hydrogen bond, as demonstrated by X-ray studies (vide infra). The most reasonable explanation for the formation of **5** appears to be the presence of small amounts of adventitious water, either in the reaction solvent or during the workup. This behavior reflects an appreciable basicity of the pyrazolate- $\kappa$ N ligand, which in turn hints that a considerable degree of steric hindering of this position is necessary to stabilize compounds such as **3b**, **3c**, and **4**.

The crystallographic determination of the structure of **5** permits the design of a more rational synthetic method. Reaction of compound **1a** with neutral  $\text{HPz}''$  in toluene affords **5** in good yields. An identical result is attained when **1b** is reacted with  $\text{HPz}$  under analogous conditions (Scheme 6). The fact that compound **5** can be indistinctly obtained from **1a** or **1b** indicates that the terminal-neutral and bridging-anionic pyrazolate positions can also be exchanged.

A related complex **6**, which contains the considerably less basic noncoordinating  $\text{BPh}_4^-$  counterion, has been prepared by reaction of **1a** with  $\text{HPz}''$  and  $\text{NaBPh}_4$  (Scheme 7). In marked contrast with **5**, **6** is insoluble in nonpolar solvents, such as toluene, and shows electrical conductivity in solution in acetone ( $\Lambda_M(20\text{ }^\circ\text{C}) = 102\ \Omega^{-1}\ \text{cm}^2\ \text{mol}^{-1}$ ) and its IR spectrum displays absorptions in the proximity of  $3370\ \text{cm}^{-1}$ , characteristic of the  $\nu(\text{N}-\text{H})$  vibration. These features support an ionic formulation for **6** in which the discrete ions are not associated through hydrogen bonding.

Both compounds **5** and **6** are fluxional in solution. In the slow exchange regime ( $< -40\text{ }^\circ\text{C}$  for **5**;  $< -20\text{ }^\circ\text{C}$  for **6**) the NMR data are indicative of the presence of two species in roughly equivalent concentrations. In the case of the bromo derivative **5**, these do not correspond to compounds **1a** or **1b**, which would result from the extrusion of  $\text{HPz}''$  or  $\text{HPz}$ , respectively, by action of  $\text{Br}^-$  (i.e., the reverse process of formation of **5**, as in the two routes of Scheme 6). The most reasonable explanation seems to be the presence in the solutions of **5** and **6** of equilibrium mixtures of rotameric isomers of the type of **A** and **B** of Chart 1. In accord with this assumption, solutions of **5**, when cooled at ca.  $-60\text{ }^\circ\text{C}$ , exhibit four Me ( $\text{Pz}''$ ) signals at  $\delta$  2.97, 2.49, 2.36, and 2.31 ppm. Comparison with the corresponding data for **3b**, **4**, and **7**<sup>6</sup> (Chart 2) suggests that the  $\text{HPz}''$  unit of the two isomers of **5** is indeed terminal.

For **6** the situation is less clear-cut since the four Me resonances appear at  $\delta$  3.01, 2.87, 2.16, and 1.77, but the results of the NOE difference experiments summarized in Scheme 7 are clearly in favor of a bridging unsubstituted pyrazolate ligand.

Despite the similarity at low temperature, the dynamic behavior of **5** and **6** diverges at higher temperatures. As shown in Figure 3, the two higher- and the two lower-field methyl pyrazole signals of **6** coalesce into distinct peaks that sharpen upon further heating. Line-shape simulation<sup>10a</sup> indicates that the two groups of Me exchange with the same rate. The independent exchange of the nuclei corresponding to the two highest field on one side and the two lowest field Me signals on the other is consistent with a restricted rotation of the  $\text{HPz}''$  ligand since it is very likely that the latter two

(12) Gloor, A.; Cadisch, M.; Bürgin-Schaller, R.; Farkas, M.; Kosciś, T.; Clerc, J. T.; Pretsch, E. *SpecTool. Hypermedia Tools for Molecular Spectroscopy*; Chemical Concepts—VCH: Weinheim, 1995.

Chart 2

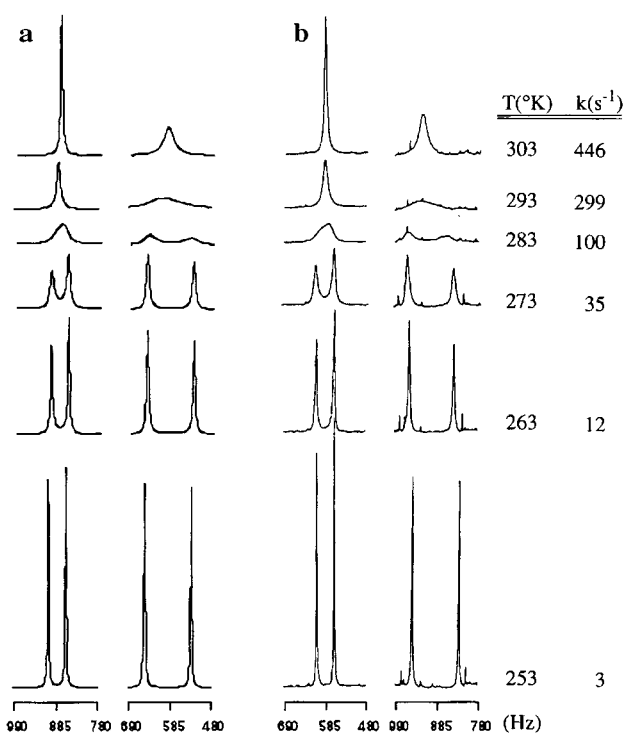
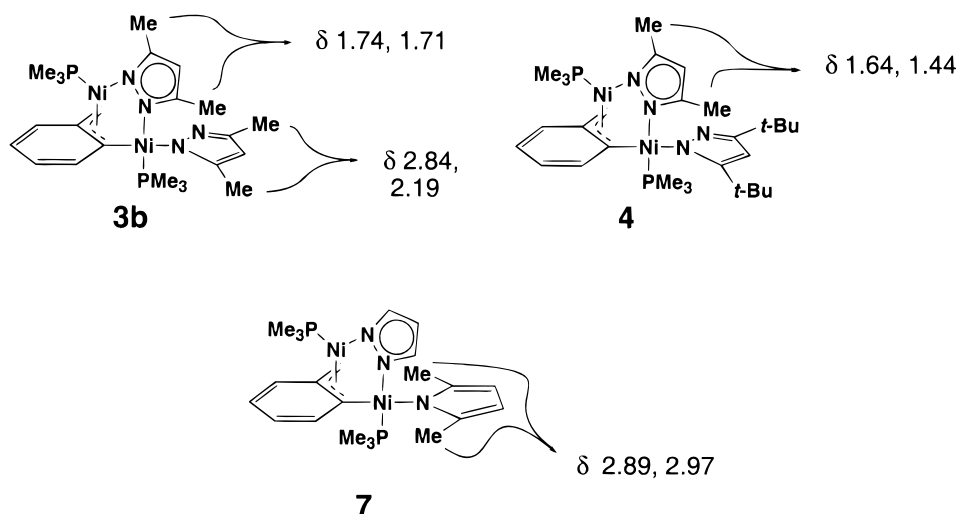


**Figure 3.** Simulated (a) and experimental (b) 300 MHz  $^1\text{H}$  NMR spectra of **6** in the methyl region at different temperatures.

correspond to the methyl groups deshielded by their proximity to the axial position of the square planar aryl Ni atom.<sup>13</sup> As for compound **5**, its dynamic behavior is somewhat more complex. A slight increase of temperature (10 °C) above the slow exchange limit (−40 °C) results in the broadening of only two of the Me pyrazole resonances, those at highest and lowest field, whereas the two central ones remain sharp. Only around 0 °C do the latter broaden, and at ca. 40 °C a broad single resonance is observed. A combination of metallotropic shift<sup>14</sup> and rotation would exchange simultaneously the four Me groups and can therefore be ruled out. Instead we propose the exchange mechanism depicted in Scheme 8, which assigns an important role

(13) Jolly, P. W.; Wilke, G. *The Organic Chemistry of Nickel*; Academic Press: New York, 1974; Vol. I, p 200.

to the  $\text{Br}^-$  group, proposing the formation of a crowded five-coordinate intermediate.<sup>15</sup>

As shown in the solid-state structure of **5**, to be discussed below, the bromide is located in a suitable position to achieve such a structure intermediate **I**. A similar intramolecular association between coordinated HPz and halide ions has been found in the complex  $\text{NiCl}_2(\text{HPz})_4$ .<sup>16</sup> Intermediate **I** can dissociate HPz to give **1a**. Full dissociation is actually not needed; the molecule of HPz may remain bound to  $\text{Br}^-$  by means of a hydrogen bond. In any case a fast N,N prototropic shift<sup>17</sup> and the reassociation of the HPz and **1a** would exchange the positions of the Me pyrazolate groups. A similar process may be proposed for the other isomer **5B**, but the corresponding intermediate **II** is less favorable on steric grounds; hence higher temperatures may be needed for its formation. Besides this dissociative exchange, rotation of the HPz' at higher temperatures would allow the interconversion of **5A** and **5B**.

**Crystal Structures of Compounds 4 and 5.** The crystal structures of **4** and **5** are shown in Figures 1 and 2. Selected bond distances and angles are summarized in Tables 1 and 2. Compound **5** crystallizes with one molecule of toluene, but since its position falls far from that of the main molecule, it has not been included in the ORTEP drawing.

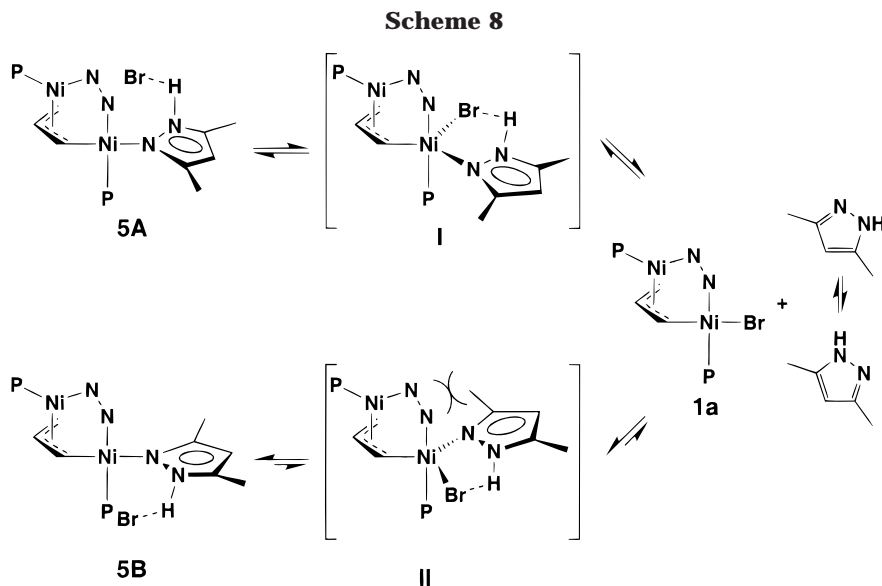
The structures of the two compounds are similar and can be related to that of **1a** by substitution of the Br atom by a HPz' in the case of **5** and a Pz\*\* in the case of complex **4**. In the latter case, a bridging Pz' group replaces the Pz ligand of **1a**. The bromine atom of **5** is associated to the molecule through a  $\text{Br}\cdots\text{H}-\text{N}$  hydrogen bond. The hydrogen atom (H121) has been located

(14) It has been proposed that the palladium complex  $[\text{PdCl}(\text{HPz})(\text{PEt}_3)_2]^+\text{BF}_4^-$  experiences a metallotropic shift of this kind. Interestingly, this species exhibits a hydrogen bond between the NH fragment of the pyrazole ligand and the counterion. See: Bushnell, G. W.; Dixon, K. R.; Eadie, K. R.; Stobart, S. R. *Inorg. Chem.* **1981**, *20*, 1545.

(15) Cross, R. J. *Adv. Inorg. Chem.* **1989**, *34*, 219.

(16) (a) Sacconi, L.; Mani, F.; Bencini, A. In *Comprehensive Coordination Chemistry*; Wilkinson, G., Gillard, R. D., McCleverty, J. A., Eds.; Pergamon Press: New York, 1987; Vol. 5; p 82. (b) Minghell, A. D.; Reimann, C. W.; Santoro, A. *Acta Crystallogr. Sect. B* **1969**, *25*, 595.

(17) Grimmet, M. R. In *Comprehensive Organic Chemistry*; Barton, D., Ollis, W. D., Haslam, E., Eds.; Pergamon Press: Oxford, 1979; Vol. 4.

**Table 1. Crystal and Refinement Data for Compounds 4 and 5**

	4	5
formula	Ni <sub>2</sub> P <sub>2</sub> N <sub>4</sub> C <sub>29</sub> H <sub>50</sub>	C <sub>28</sub> H <sub>43</sub> N <sub>4</sub> P <sub>2</sub> Ni <sub>2</sub> Br
mol wt	634.1	694.9
cryst syst	triclinic	monoclinic
space group	<i>P</i> $\bar{1}$	<i>P</i> 2 <sub>1</sub> / <i>c</i> (No. 14)
cell dimens		
<i>a</i> , Å	10.059(5)	10.421(6)
<i>b</i> , Å	10.221(4)	10.388(2)
<i>c</i> , Å	18.695(6)	31.116(6)
$\alpha$ , deg	100.95(3)	
$\beta$ , deg	87.98(4)	99.61(3)
$\gamma$ , deg	119.04(4)	
<i>Z</i>	2	4
<i>V</i> , Å <sup>3</sup>	1646(1)	3321(2)
<i>D</i> <sub>calcd</sub> , g cm <sup>-3</sup>	1.28	1.39
<i>F</i> (000)	676	1440
temp, K	225	295
diffractometer	Enraf-Nonius	Enraf-Nonius
radiation	graphite-monochromated Mo K $\alpha$	graphite-monochromated Mo K $\alpha$
	( $\lambda = 0.71069$ Å)	( $\lambda = 0.71069$ Å)
$\mu$ (Mo K $\alpha$ ), cm <sup>-1</sup>	12.7	24.5
cryst dimens, mm	0.1 × 0.15 × 0.25	0.3 × 0.25 × 0.3
2 $\theta$ range, deg	2–50	1–50
scan technique	$\omega/2\theta$	$\omega/2\theta$
data collected	(–11, –12, 0) to (11, 12, 22)	(–12, 00) to (12, 12, 37)
unique data	5774	5834
observed reflections, <i>I</i> > 3 $\sigma$ ( <i>I</i> )	3865	3416
<i>R</i> <sub>int</sub> (%)	1.2	1.8
decay	≤ 1%	
standard reflns	3/67	3/67
weighting scheme	unit	unit
<i>R</i> = $\sum  \Delta^2 F  / \sum  F_0 $	3.7	7.0
<i>R</i> <sub>w</sub> = $(\sum w \Delta^2 F / \sum w  F_0 )^{1/2}$	4.1	7.5
max shift/error	0.02	2.4
abs corr range	0.81–1.11	0.94–1.08

in the electron density map at 2.39 and 0.83 Å from the Br and N12 atoms, respectively. The three atoms depart slightly from linearity, forming an angle of 170.7°. This arrangement results in a Br–N distance of 3.15 Å, very close to that expected for a typical Br⋯H–N hydrogen bond,<sup>18</sup> and brings the bromine atom in the proximity

**Table 2. Selected Bonds Distances and Angles for Compound 4**

Bond Distances (Å)			
Ni1–Ni2	2.778(2)	Ni2–C1	2.137(4)
Ni1–P1	2.171(2)	Ni2–C2	2.126(6)
Ni1–N11	1.912(4)	Ni2–C7	1.929(7)
Ni1–N21	1.939(5)	N11–N12	1.377(4)
Ni1–C1	1.931(5)	N21–N22	1.377(4)
Ni2–P2	2.137(2)	C1–C2	1.424(7)
Ni2–N22	1.904(5)	C2–C7	1.444(6)
Bond Angles (deg)			
N21–Ni1–C1	88.9(2)	P2–Ni2–C7	89.7(2)
N11–Ni1–C1	169.8(2)	P2–Ni2–C2	128.3(2)
N11–Ni1–N21	93.5(2)	P2–Ni2–C1	162.1(2)
P1–Ni1–C1	89.3(2)	P2–Ni2–N22	106.1(2)
P1–Ni1–N21	173.8(2)	Ni1–N21–N22	114.6(3)
P1–Ni1–N11	87.2(1)	Ni2–N22–N21	108.1(3)
Ni1–N11–N12	113.9(3)	Ni1–C1–Ni2	86.0(2)
Ni1–N11–C15	136.5(4)	Ni2–C1–C2	70.1(3)
Ni1–N21–C26	137.7(3)	Ni1–C1–C2	133.0(4)
Ni2–N22–C24	143.2(4)	Ni2–C2–C1	70.9(3)
C2–Ni2–C7	41.4(2)	C1–C2–C7	117.2(5)
C1–Ni2–C7	73.9(2)	Ni2–C2–C7	62.0(3)
C1–Ni2–C2	39.0(2)	Ni2–C7–C2	76.7(3)

of Ni1, precisely above its axial coordination site, but not close enough to postulate a bonding interaction. These atoms are 3.82 Å apart, far beyond bonding distance.

The terminal Pz\*\* or HPz' groups of both compounds are approximately coplanar, with the C<sub>7</sub>H<sub>6</sub> unit and perpendicular to the Ni1 coordination plane. As discussed before, this disposition allows two possible conformations for the terminal rings. One has the uncoordinated N atom on the same side of the molecule as the CH<sub>2</sub> group, whereas in the other these atoms are situated on opposite sides. Interestingly enough, compounds **4** and **5** exhibit opposite conformations in the solid state.

The central core of these compounds is very similar to that of **1a**. Like the latter, **4** and **5** have surprisingly short Ni2–C1 bond (**4**, 2.137 Å; **5**, 2.10 Å) as compared to the related mononuclear complex Ni(Br)(PMe<sub>3</sub>)( $\eta^3$ -CH<sub>2</sub>C<sub>6</sub>H<sub>4</sub>-*o*-CH<sub>3</sub>)<sup>19</sup> (2.318 Å). This short Ni–C distance enforces the proximity of the two Ni atoms, making the

(18) Greenwood, N. N.; Earnshaw, A. *Chemistry of the Elements*; Pergamon Press: Oxford, 1984.

(19) Carmona, E.; Marín, J. M.; Paneque, M.; Poveda, M. L. *Organometallics* **1987**, *6*, 1757.

Ni–Ni distances shorter than twice the van der Waals radius (3.2 Å).<sup>20</sup> The possibility of a weak bonding interaction has been discussed elsewhere.<sup>6</sup> Here we would only like to remark that the shortest Ni–Ni distance corresponds to compound **4**, in which the bulky Pz\*\* and Pz' groups surround the Ni atoms. This suggests that electronic factors may have some influence in the values of the Ni–Ni distance. For example, the delocalization of the positive charge in compound **5** might induce some electrostatic repulsion between the Ni atoms, thus increasing the Ni–Ni distance.

### Concluding Remarks

The synthesis of compounds **3b**, **3c**, and **4**, which contain bridging and terminal pyrazolate ligands, has allowed the detection of different types of dynamic processes, namely, N,N metal shift, rotation of the terminal ligand, and bridging–terminal and intermolecular pyrazolate exchange. In addition to these processes, the stereoselective exchange of the HPz'' ligand of compound **5** mediated by the bromide counterion has been observed. Compounds **5** and **6** exist in solution as a mixture of two possible rotational isomers (**5A–5B** and **6A–6B**, respectively), while for **3b**, **3c**, and **4** only one isomer has been found, even when the rotation of the terminal ligand is a relatively slow process. This observation suggests that they experience a very fast N,N metal shift in solution, which renders the average spectrum of both conformers, even at low temperatures. This process is much slower or does not take place at all in the case of compounds **5** and **6**, in which the uncoordinated N atom is blocked by a H atom. In contrast with this fast N,N shift, the rotation of the bridging ligand, a process that exchanges the relative position of the latter with respect to the metal atoms (i.e., Ni(1)–N(1)–N(2)–Ni(2) ⇌ Ni(1)–N(2)–N(1)–Ni(2)), and that has been detected previously in complexes of type **1**,<sup>6</sup> is too slow to be observed, even under conditions of magnetization transfer.

### Experimental Section

Microanalyses were by Pascher, Microanalytical Laboratory, Remagen, Germany, and the Analytical Service of the University of Seville. The spectroscopic instruments used were Perkin-Elmer models 577 and 684 for IR spectra and Varian XL-200, Bruker AMX-300, and AMX-500 for NMR spectroscopy. The <sup>13</sup>C resonance of the solvent was used as an internal standard, but chemical shifts are reported with respect to SiMe<sub>4</sub>. The <sup>13</sup>C{<sup>1</sup>H} NMR assignments were helped in most cases with the use of gate decoupling techniques. <sup>31</sup>P{<sup>1</sup>H} NMR shifts are referenced to external 85% H<sub>3</sub>PO<sub>4</sub>. All preparations and other operations were carried out under oxygen-free nitrogen following conventional Schlenk techniques. Solvents were dried and degassed before use. The petroleum ether used had a boiling point of 40–60 °C. Lithium pyrazolate was obtained by reacting n-BuLi with pyrazole, and NaCp from NaH and freshly cracked dicyclopentadiene. Compounds **1a–c**<sup>6</sup> and **2**<sup>8</sup> were prepared according to published methods.

**Synthesis of Ni<sub>2</sub>(PMe<sub>3</sub>)<sub>2</sub>(N<sub>2</sub>CHR<sub>2</sub>)(μ<sub>2</sub>-η<sup>3</sup>:η<sup>1</sup>-CH<sub>2</sub>-o-C<sub>6</sub>H<sub>4</sub>)-(μ<sub>2</sub>-N<sub>2</sub>C<sub>3</sub>HR<sub>2</sub>) (R = Me, **3b**; R = Bu<sup>t</sup>, **3c**).** Complexes **3b** and **3c** have been prepared by reacting compound **2** with the corresponding thallium pyrazolate salt, following the procedure described below for complex **3b**: EtOTl (2 mmol, 4 mL of a

0.5 M solution in THF) was added to a cold (–40 °C) solution of 3,5-dimethylpyrazole (0.2 g, 2 mmol). After removing the cold bath the mixture was allowed to reach room temperature and added to a stirred solution of **2** (0.6 g, 1 mmol) in THF (50 mL) cooled at –80 °C. The resulting mixture was warmed to room temperature and then further stirred for 30 min. The solvent was removed under vacuum and the residue extracted with Et<sub>2</sub>O. After centrifugation and partial concentration of the solution, cooling at –30 °C provided orange crystals of the compound **3b** in 93% yield.

The more soluble complex **3c** was similarly prepared and crystallized from petroleum ether as red crystals in 36% yield.

**Ni<sub>2</sub>(PMe<sub>3</sub>)<sub>2</sub>(N<sub>2</sub>C<sub>3</sub>HMe<sub>2</sub>)(μ<sub>2</sub>-η<sup>3</sup>:η<sup>1</sup>-CH<sub>2</sub>-o-C<sub>6</sub>H<sub>4</sub>)(μ<sub>2</sub>-N<sub>2</sub>C<sub>3</sub>HMe<sub>2</sub>) (**3b**).** Anal. Calcd for C<sub>23</sub>H<sub>38</sub>N<sub>4</sub>P<sub>2</sub>Ni<sub>2</sub>: C, 50.2; H, 6.9; N, 10.2. Found: C, 50.2; H, 7.0; N, 10.1.

<sup>1</sup>H NMR (CD<sub>2</sub>Cl<sub>2</sub>, 20 °C): δ 0.78 (d, 9 H, <sup>2</sup>J<sub>HP</sub> = 10.5 Hz, PMe<sub>3</sub>), 1.46 (d, 9 H, <sup>2</sup>J<sub>HP</sub> = 8.9 Hz, PMe<sub>3</sub>), 1.64, 1.71 (s, s, 3 H, 3 H, Me pyraz), 2.02 (dd, 1 H, <sup>2</sup>J<sub>HH</sub> = 3.7, <sup>3</sup>J<sub>HP</sub> = 8.2 Hz, CH<sub>2</sub>), 2.12 (pt, 1 H, <sup>2</sup>J<sub>HH</sub> ≈ <sup>3</sup>J<sub>HP</sub> = 4.3 Hz, CH<sub>2</sub>), 2.19, 2.84 (s, s, 3 H, 3 H, Me pyraz), 5.33, 5.61 (s, s, 1 H, 1 H, H pyraz), 6.83 (m, 1H, aromatic), 7.03 (m, 2 H, aromatics), 7.84 (m, 1 H, aromatic). <sup>31</sup>P{<sup>1</sup>H} NMR (CD<sub>2</sub>Cl<sub>2</sub>, 20 °C): AX spin system, δ<sub>A</sub> = –10.9, δ<sub>X</sub> = –8.4, J<sub>AX</sub> = 5 Hz. <sup>13</sup>C{<sup>1</sup>H} NMR (CD<sub>2</sub>Cl<sub>2</sub>, 20 °C): δ 11.7 (s, Me pyraz), 13.5 (d, <sup>1</sup>J<sub>CP</sub> = 29 Hz, PMe<sub>3</sub>), 13.6, 14.0, 14.8 (s, Me pyraz), 16.4 (d, <sup>1</sup>J<sub>CP</sub> = 27 Hz, PMe<sub>3</sub>), 29.3 (d, <sup>2</sup>J<sub>CP</sub> = 12, <sup>1</sup>J<sub>CH</sub> = 151 Hz, CH<sub>2</sub>), 102.4, 103.6 (s, C(4)H pyraz), 123.7, 124.3, 128.4, 144.9 (s, CH aromatics), 126.2 (dd, <sup>2</sup>J<sub>CP</sub> = 20 and 40 Hz, C<sub>q</sub> arom-Ni), 127.9 (d, <sup>2</sup>J<sub>CP</sub> = 3 Hz, C<sub>q</sub> arom), 147.4, 150.3, 150.4 (s, 2, 1, and 1 C<sub>q</sub> pyraz).

**Ni<sub>2</sub>(PMe<sub>3</sub>)<sub>2</sub>(N<sub>2</sub>C<sub>3</sub>H<sup>t</sup>Bu<sub>2</sub>)(μ<sub>2</sub>-η<sup>3</sup>:η<sup>1</sup>-CH<sub>2</sub>-o-C<sub>6</sub>H<sub>4</sub>)(μ<sub>2</sub>-N<sub>2</sub>C<sub>3</sub>H<sup>t</sup>Bu<sub>2</sub>) (**3c**).** Anal. Calcd for C<sub>35</sub>H<sub>62</sub>N<sub>4</sub>P<sub>2</sub>Ni<sub>2</sub>: C, 58.8; H, 8.7; N, 7.8. Found: C, 58.8; H, 8.8; N, 7.3.

<sup>1</sup>H NMR (CD<sub>2</sub>Cl<sub>2</sub>, 20 °C): δ 0.60 (d, 9 H, <sup>2</sup>J<sub>HP</sub> = 10.7 Hz, PMe<sub>3</sub>), 0.92, 1.27, 1.33 (s, s, s, 9 H, 9 H, 9 H, CMe<sub>3</sub> pyraz), 1.58 (d, 9 H, <sup>2</sup>J<sub>HP</sub> = 8.4 Hz, PMe<sub>3</sub>), 2.0 (s, 9 H, CMe<sub>3</sub>), 2.16 (pt, 1 H, <sup>2</sup>J<sub>HH</sub> ≈ <sup>3</sup>J<sub>HP</sub> = 4.2 Hz, CH<sub>2</sub>), 5.52, 5.67 (s, s, 1 H, 1 H, H(4) pyraz), 6.70 (d, 1 H, J<sub>HH</sub> = 7.6 Hz, aromatic), 6.87 (m, 2 H, aromatics), 7.32 (d, 1 H, <sup>3</sup>J<sub>HH</sub> = 8.0 Hz, aromatic). <sup>31</sup>P{<sup>1</sup>H} NMR (CD<sub>2</sub>Cl<sub>2</sub>, 20 °C): AX spin system, δ<sub>A</sub> = –17.3, δ<sub>X</sub> = –15.2, J<sub>AX</sub> = 5 Hz. <sup>13</sup>C{<sup>1</sup>H} NMR (CD<sub>2</sub>Cl<sub>2</sub>, 20 °C): δ 14.3 (d, <sup>1</sup>J<sub>CP</sub> = 29 Hz, PMe<sub>3</sub>), 17.1 (d, <sup>1</sup>J<sub>CP</sub> = 27 Hz, PMe<sub>3</sub>), 29.8 (d, <sup>2</sup>J<sub>CP</sub> = 14, <sup>1</sup>J<sub>CH</sub> = 149 Hz, CH<sub>2</sub>), 31.1, 31.3, 31.6, 33.3 (s, CMe<sub>3</sub> pyraz), 32.1, 32.3, 32.4, (s, CMe<sub>3</sub>), 96.9, 101.0 (s, C(4)H pyraz), 121.3 (dd, <sup>2</sup>J<sub>CP</sub> = 20 and 48 Hz, C<sub>q</sub> arom-Ni), 122.9, 124.7, 128.1, 143.7 (s, CH aromatics), 126.7 (d, <sup>2</sup>J<sub>CP</sub> = 5 Hz, C<sub>q</sub> arom), 159.8, 161.3, 161.7, 165.3 (s, s, s, and d, J<sub>CP</sub> = 3 Hz, C<sub>q</sub> pyraz).

**Synthesis of Ni<sub>2</sub>(PMe<sub>3</sub>)<sub>2</sub>(N<sub>2</sub>C<sub>3</sub>H<sup>t</sup>Bu<sub>2</sub>)(μ<sub>2</sub>-η<sup>3</sup>:η<sup>1</sup>-CH<sub>2</sub>-o-C<sub>6</sub>H<sub>4</sub>)(μ<sub>2</sub>-N<sub>2</sub>C<sub>3</sub>HMe<sub>2</sub>) (**4**).** A solution of 3,5-di-*tert*-butylpyrazole (0.12 g, 0.65 mmol) in THF (10 mL) cooled at –40 °C was treated with EtOTl (0.65 mmol, 1.2 mL of a 0.54 M solution in THF). When the mixture reached room temperature, it was added to a cooled (–80 °C) solution of complex **1b** (0.35 g, 0.65 mmol) in Et<sub>2</sub>O (40 mL). The cooling bath was removed, and after stirring at room temperature for 3 h, the reaction mixture was taken to dryness and the residue extracted with toluene. The resulting suspension was centrifuged, the solution evaporated under reduced pressure, and the residue extracted with petroleum ether. After filtration, partial evaporation of the filtrate, and cooling at –30 °C compound **4** was isolated as orange crystals in 50% yield. It can be recrystallized from Me<sub>2</sub>CO–petroleum ether (1:1) as orange plates.

Compound **4** was also prepared by the reaction of complex **1c** with thallium 3,5-dimethylpyrazole in 40% yield.

Anal. Calcd for C<sub>29</sub>H<sub>50</sub>N<sub>4</sub>P<sub>2</sub>Ni<sub>2</sub>: C, 54.9; H, 7.9. Found: C, 55.0; H, 7.9. <sup>1</sup>H NMR (CD<sub>2</sub>Cl<sub>2</sub>, 20 °C): δ 0.63 (d, 9 H, <sup>2</sup>J<sub>HP</sub> = 9.5 Hz, PMe<sub>3</sub>), 1.27 (s, 9 H, CMe<sub>3</sub> pyraz), 1.44 (d, 9 H, <sup>2</sup>J<sub>HP</sub> = 8.8 Hz, PMe<sub>3</sub>), 1.44, 1.67 (s, s, 3 H, 3 H, Me pyraz), 1.74 (s, 9 H, CMe<sub>3</sub> pyraz), 2.06 (dd, 1 H, <sup>2</sup>J<sub>HH</sub> = 3.7, <sup>3</sup>J<sub>HP</sub> = 8.6 Hz, CH<sub>2</sub>), 2.11 (pt, 1 H, <sup>2</sup>J<sub>HH</sub> ≈ <sup>3</sup>J<sub>HP</sub> = 3.7 Hz, CH<sub>2</sub>), 5.26 (s, 1 H, H(4) pyraz), 5.66 (d, 1 H, <sup>3</sup>J<sub>HH</sub> = 0.5 Hz, H(4) pyraz), 6.77 (m, 1H, aromatic), 7.01 (m, 2 H, aromatics), 8.04 (m, 1 H, aromatic).

$^{31}\text{P}\{^1\text{H}\}$  NMR ( $\text{CD}_2\text{Cl}_2$ , 20 °C): AX spin system,  $\delta_{\text{A}} = -12.6$ ,  $\delta_{\text{X}} = -11.3$ ,  $J_{\text{AX}} = 4$  Hz.  $^{13}\text{C}\{^1\text{H}\}$  NMR ( $\text{CD}_2\text{Cl}_2$ , 20 °C):  $\delta$  11.6 (s, Me pyraz), 13.6 (d,  $^1J_{\text{CP}} = 28$  Hz,  $\text{PMe}_3$ ), 16.4 (d,  $^1J_{\text{CP}} = 27$  Hz,  $\text{PMe}_3$ ), 30.5 (d,  $^2J_{\text{CP}} = 12$  Hz,  $\text{CH}_2$ ), 30.5 (s,  $\text{CMe}_3$  pyraz), 31.6 (s,  $\text{CMe}_3$  pyraz), 32.1 (s,  $\text{CMe}_3$  pyraz), 32.3 (s, Me pyraz), 32.4 (s,  $\text{CMe}_3$  pyraz), 96.2 (s, C(4) H Bu $^t_2$ ), 103.9 (d,  $J_{\text{CP}} = 2$  Hz, C(4)H Me $_2$ pyraz), 122.4 (dd,  $^2J_{\text{CP}} = 20$  and 42 Hz,  $\text{C}_q$  arom-Ni), 122.8, 123.9, 128.5, 146.4 (s, CH aromatics), 128.5 (d,  $^2J_{\text{CP}} = 5$  Hz,  $\text{C}_q$  arom), 147.1, 151.1, 160.2, 160.7 (d, s, s, and s,  $J_{\text{CP}} = 3$  Hz,  $\text{C}_q$  pyraz).

**Synthesis of  $[\text{Ni}_2(\text{PMe}_3)_2(\text{HN}_2\text{CHMe}_2)(\mu_2\text{-}\eta^3\text{-}\eta^1\text{-CH}_2\text{-}\sigma\text{-C}_6\text{H}_4)(\mu_2\text{-N}_2\text{C}_3\text{H}_3)]\text{Br} \cdot \text{C}_7\text{H}_8$  (5).** Method a. *n*-BuLi (1 mmol, 0.62 mL of a 1.6 M solution in hexanes) was added to a cold (−40 °C) solution of 3,5-dimethylpyrazole (0.1 g, 1 mmol) in THF (10 mL). After removing the cooling bath the mixture was allowed to reach room temperature and added to a solution of complex **1a** (0.5 g, 1 mmol) in THF (50 mL) cooled at −60 °C. The suspension was stirred at room temperature for 2 h. The solvent was removed under vacuo, the residue extracted with toluene, and the resulting suspension centrifuged. The solution was again taken to dryness and the residue extracted with Et $_2$ O. After filtration, partial concentration of the solvent, and cooling at −30 °C compound **5** was isolated as red crystals in 32% yield.

Compound **5** may be prepared in 43% yield by the alternative reaction of **1b** with lithium pyrazolate.

**Method b.** A solution of 3,5-dimethylpyrazole (0.1 g, 1 mmol) in 10 mL of THF was added to a stirred solution of compound **1a** (0.5 g, 1 mmol) in 30 mL of THF. The resulting mixture was stirred at room temperature for 2 h. The solvent was removed under vacuum and the residue extracted with toluene. After filtration and concentration of the solution, cooling at −30 °C furnished red crystals of compound **5** in 63% yield. The same product could be also obtained in 39% yield by the reaction of compound **1b** with pyrazole.

Anal. Calcd for  $\text{C}_{28}\text{H}_{43}\text{N}_4\text{BrP}_2\text{Ni}_2$ : C, 48.4; H, 6.2; N, 8.1. Found: C, 48.5; H, 6.3, N, 8.2.

**5a:**  $^1\text{H}$  NMR ( $\text{CD}_2\text{Cl}_2$ , −40 °C)  $\delta$  0.66 (d, 9 H,  $^2J_{\text{HP}} = 10.4$  Hz,  $\text{PMe}_3$ ), 1.41 (d, 9 H,  $^2J_{\text{HP}} = 9.5$  Hz,  $\text{PMe}_3$ ), 2.32, 2.40 (m, m, 1 H, 1 H,  $\text{CH}_2$ ), 2.40, 2.97 (s, s, 3 H, 3 H, Me pyraz), 5.86 (s, 1 H, H(4) pyraz), 6.00 (s, 1 H, H(4) Me $_2$ pyraz), 6.60 (d, 1 H,  $^3J_{\text{HH}} = 2.0$  Hz, H pyraz), 6.83 (m, 1 H, aromatic), 6.87 (bs, 1 H, H pyraz), 7.0–7.2 (m, 2 H, aromatics), 8.08 (d, 1 H,  $^3J_{\text{HH}} = 8.0$  Hz, aromatic), 14.1 (bs, 1 H, NH pyraz);  $^{31}\text{P}\{^1\text{H}\}$  NMR ( $\text{CD}_2\text{Cl}_2$ , −40 °C) AX spin system,  $\delta_{\text{A}} = -10.9$ ,  $\delta_{\text{X}} = -9.2$ ,  $J_{\text{AX}} = 6$  Hz.

**5b:**  $^1\text{H}$  NMR ( $\text{CD}_2\text{Cl}_2$ , −40 °C)  $\delta$  0.75 (d, 9 H,  $^2J_{\text{HP}} = 10.4$  Hz,  $\text{PMe}_3$ ), 1.36 (d, 9 H,  $^2J_{\text{HP}} = 9.2$  Hz,  $\text{PMe}_3$ ), 2.31, 2.86 (s, s, 3 H, 3 H, Me pyraz), 2.40 (m, 1 H,  $\text{CH}_2$ ), 3.40 (pt, 1 H,  $^2J_{\text{HH}} \approx ^3J_{\text{HP}} = 3.7$  Hz,  $\text{CH}_2$ ), 5.80 (s, 1 H, H(4) pyraz), 5.91 (s, 1 H, H(4) Me $_2$ pyraz), 6.83 (m, 1H, aromatic), 6.89 (d, 1 H,  $^3J_{\text{HH}} = 2.0$  Hz, H pyraz), 7.0–7.2 (m, 2 H, aromatic), 8.33 (d, 1 H,  $^3J_{\text{HH}} = 7.4$  Hz, aromatic), 15.0 (bs, 1 H, NH pyraz);  $^{31}\text{P}\{^1\text{H}\}$  NMR ( $\text{CD}_2\text{Cl}_2$ , −40 °C) AX spin system,  $\delta_{\text{A}} = -10.5$ ,  $\delta_{\text{X}} = -8.5$ ,  $J_{\text{AX}} = 6$  Hz.

**5a,b:**  $^{13}\text{C}\{^1\text{H}\}$  NMR ( $\text{CD}_2\text{Cl}_2$ , −40 °C)  $\delta$  11.3, 11.4 (s, Me *exo* pyraz), 14.0 (d,  $^1J_{\text{CP}} = 32$  Hz,  $\text{PMe}_3$ ), 14.6 (d,  $^1J_{\text{CP}} = 30$  Hz,  $\text{PMe}_3$ ), 14.7, 15.5 (s, Me *endo* pyraz), 15.8 (d,  $^1J_{\text{CP}} = 27$  Hz,  $\text{PMe}_3$ ), 15.9 (d,  $^1J_{\text{CP}} = 28$  Hz,  $\text{PMe}_3$ ), 32.3 (d,  $^2J_{\text{CP}} = 10$  Hz,  $\text{CH}_2$ ), 36.1 (d,  $^2J_{\text{CP}} = 10$  Hz,  $\text{CH}_2$ ), 103.6, 103.7 (s, C(4)H Me $_2$ pyraz), 106.0, 106.2 (s, C(4)H pyraz), 113.4 (dd,  $^2J_{\text{CP}} = 16$  and 41 Hz,  $\text{C}_q$  arom-Ni), 118.5 (dd,  $^2J_{\text{CP}} = 20$ , 43 Hz,  $\text{C}_q$  arom-Ni), 123.8, 124.0, 124.8, 125.4, 129.1, 129.4, 145.0, 146.9 (s, CH aromatics), 126.3 (d,  $^2J_{\text{CP}} = 5$  Hz,  $\text{C}_q$  arom), 127.2 (d,  $^2J_{\text{CP}} = 6$  Hz,  $\text{C}_q$  arom), 137.3, 138.2, 140.5, 141.3 (s, CH pyraz), 143.0, 143.5, 148.1, 149.7 (s,  $\text{C}_q$  pyraz).

**Synthesis of  $[\text{Ni}_2(\text{PMe}_3)_2(\text{HN}_2\text{CHMe}_2)(\mu_2\text{-}\eta^3\text{-}\eta^1\text{-CH}_2\text{-}\sigma\text{-C}_6\text{H}_4)(\mu_2\text{-N}_2\text{C}_3\text{H}_3)]\text{BPh}_4 \cdot 0.5\text{Me}_2\text{CO}$  (6).** NaBPh $_4$  (0.42 g, 1.22 mmol) and 3,5-dimethylpyrazole (0.12 g, 1.22 mmol) were dissolved in THF (10 mL), and the solution was cooled at 0 °C

**Table 3. Selected Bonds Distances and Angles for Compound 5**

Bond Distances (Å)			
Ni1–Ni2	2.853(2)	Ni2–C1	2.10 (1)
Ni1–P1	2.173(4)	Ni2–C2	2.08 (1)
Ni1–N11	1.924(8)	Ni2–C7	1.91 (1)
Ni1–N21	1.920(8)	N11–N12	1.33 (1)
Ni1–C1	1.90 (1)	N21–N22	1.38 (1)
Ni2–P2	2.146(3)	C1–C2	1.46 (1)
Ni2–N22	1.902(9)	C2–C7	1.42 (2)
Bond Angles (deg)			
N21–Ni1–C1	90.2(4)	P2–Ni2–C7	92.5(4)
N11–Ni1–C1	170.6(4)	P2–Ni2–C2	129.5(4)
N11–Ni1–N21	88.9(4)	P2–Ni2–C1	166.7(3)
P1–Ni1–C1	87.7(4)	P2–Ni2–N22	102.5(3)
P1–Ni1–N21	176.6(3)	Ni1–N21–N22	118.3(6)
P1–Ni1–N11	92.9(3)	Ni2–N22–N21	106.5(6)
Ni1–Ni1–N12	122.6(7)	Ni1–C1–Ni2	90.8(4)
Ni1–Ni1–C15	131.3(8)	Ni2–C1–C2	68.7(6)
Ni1–N21–C25	135.7(7)	Ni1–C1–C2	132.6(8)
Ni2–N22–C23	142.3(7)	Ni2–C2–C1	70.5(6)
C2–Ni2–C7	41.3(5)	C1–C2–C7	117.1(1)
C1–Ni2–C7	74.9(5)	Ni2–C2–C7	63.1(6)
C1–Ni2–C2	40.8(4)	Ni2–C7–C2	75.6(7)

and then added to a solution of complex **1a** (0.62 g, 1.22 mmol) cooled also at 0 °C. The resulting mixture was warmed to room temperature and then further stirred for 15 min. After evaporation of the solvent the residue was extracted twice with  $\text{CH}_2\text{Cl}_2$  and centrifuged. The clear solution was evaporated and the residue crystallized from an acetone–petroleum ether mixture at 0 °C. Compound **6** was isolated as red crystals in 92% yield.

Anal. Calcd for  $\text{C}_{45}\text{H}_{55}\text{N}_4\text{BP}_2\text{Ni}_2$ : C, 64.1; H, 6.7. Found: C, 64.0; H, 6.8.

**6a:**  $^1\text{H}$  NMR ( $\text{CD}_2\text{Cl}_2$ , −20 °C)  $\delta$  0.47 (d, 9 H,  $^2J_{\text{HP}} = 10.1$  Hz,  $\text{PMe}_3$ ), 1.38 (d, 9 H,  $^2J_{\text{HP}} = 9.2$  Hz,  $\text{PMe}_3$ ), 1.77, 3.01 (s, s, 3 H, 3 H, Me pyraz), 5.89 (s, 1 H, H(4) pyraz), 5.98 (s, 1 H, H(4) Me $_2$ pyraz), 6.22 (d, 1 H,  $^3J_{\text{HH}} = 2.0$  Hz, H pyraz), 6.96 (1 H, H pyraz, partially obscured by a BPh $_4$  resonance), 7.95 (d, 1 H,  $^3J_{\text{HH}} = 8.8$  Hz, aromatic), 9.92 (bs, 1 H, NH pyraz);  $^{31}\text{P}\{^1\text{H}\}$  NMR ( $\text{CD}_2\text{Cl}_2$ , −20 °C) AX spin system,  $\delta_{\text{A}} = -11.8$ ,  $\delta_{\text{X}} = -10.5$ ,  $J_{\text{AX}} = 6$  Hz.

**6b:**  $^1\text{H}$  NMR ( $\text{CD}_2\text{Cl}_2$ , −20 °C)  $\delta$  0.63 (d, 9 H,  $^2J_{\text{HP}} = 10.1$  Hz,  $\text{PMe}_3$ ), 1.37 (d, 9 H,  $^2J_{\text{HP}} = 9.2$  Hz,  $\text{PMe}_3$ ), 2.16, 2.87 (s, s, 3 H, 3 H, Me pyraz), 5.87 (s, 1 H, H(4) pyraz), 5.96 (s, 1 H, H(4) Me $_2$ pyraz), 6.52 (d, 1 H,  $^3J_{\text{HH}} = 1.8$  Hz, H pyraz), 6.83 (1 H, H pyraz, partially obscured by a BPh $_4$  resonance), 8.23 (d, 1 H,  $^3J_{\text{HH}} = 8.1$  Hz, aromatic), 8.55 (bs, 1 H, NH pyraz);  $^{31}\text{P}\{^1\text{H}\}$  NMR ( $\text{CD}_2\text{Cl}_2$ , −20 °C) AX spin system,  $\delta_{\text{A}} = -10.6$ ,  $\delta_{\text{X}} = -9.4$ ,  $J_{\text{AX}} = 4$  Hz.

**6a,b:**  $^{13}\text{C}\{^1\text{H}\}$  NMR ( $\text{CD}_2\text{Cl}_2$ , −20 °C)  $\delta$  11.5, 11.8 (s, Me *exo* pyraz), 14.1 (d,  $^1J_{\text{CP}} = 30$  Hz,  $\text{PMe}_3$ ), 14.3 (d,  $^1J_{\text{CP}} = 30$  Hz,  $\text{PMe}_3$ ), 16.0 (d,  $^1J_{\text{CP}} = 28$  Hz,  $\text{PMe}_3$ ), 16.1 (d,  $^1J_{\text{CP}} = 28$  Hz,  $\text{PMe}_3$ ), 14.8, 15.8 (s, Me *endo* pyraz), 33.3 (d,  $^2J_{\text{CP}} = 12$  Hz,  $\text{CH}_2$ ), 35.2 (d,  $^2J_{\text{CP}} = 12$  Hz,  $\text{CH}_2$ ), 104.1, 104.4 (s, C(4)H pyraz), 107.1, 107.0 (s, C(4)H Me $_2$ pyraz), 110.9 (dd,  $^2J_{\text{CP}} = 21$  and 41 Hz,  $\text{C}_q$  arom-Ni), 115.8 (dd,  $^2J_{\text{CP}} = 19$  and 42 Hz,  $\text{C}_q$  arom-Ni), 123.7, 124.6, 125.9, 130.1, 144.2, 144.9 (s, CH aromatics), 126.2 (d,  $^2J_{\text{CP}} = 5$  Hz,  $\text{C}_q$  arom), 127.1 (d,  $^2J_{\text{CP}} = 5$  Hz,  $\text{C}_q$  arom), 137.6, 137.8, 141.5, 142.2 (s, CH pyraz), 144.6, 144.7, 150.0, 151.9 (s,  $\text{C}_q$  pyraz).

**X-ray Structure Determination of Compounds 4 and 5.** A summary of the fundamental crystal data is given in Table 3. A crystal of prismatic shape was coated with an epoxy resin and mounted in a Kappa diffractometer. The cell dimensions were refined by least-squares fitting of the  $\theta$  values of the 25 reflections with a  $2\theta$  range of 13–30° (**4**) and 13–24° (**5**). The data collection was performed at 225 K for **4**. The intensities were corrected for Lorentz and polarization effects. Scattering factors for neutral atoms and anomalous dispersion corrections for Br, Ni, and Br were taken from the International Tables



for X-ray Crystallography.<sup>21a</sup> The structure was solved by Patterson and Fourier methods. An empirical absorption correction<sup>21b</sup> was applied at the end of the isotropic refinements. Because of the nonresolvable disorder due to the thermal motion involving the Br atoms and the toluene molecules in compound **5**, the *R* values and the maximum shift/error are higher than usual. A final refinement was undertaken with unit weight and anisotropic thermal motion for the non-hydrogen atoms. The hydrogen atoms were included with fixed isotropic contributions at their calculated positions. No trend in  $\Delta F$  vs  $F_0$  or  $\sin \theta/\lambda$  was observed. Final difference

---

(21) (a) *International Tables for X-ray Crystallography*, Kynoch Press: Birmingham, U.K., 1974; Vol. IV, p 72. (b) Walker, N.; Stuart, D. *Acta Crystallogr.* **1983**, *A39*, 158. (c) Stewart, J. M. *The X-Ray 80 System*, Computer Science Center, University of Maryland: College Park, MD, 1985.

synthesis showed no significant electron density. Most of the calculations were carried out with the X-ray 80 system.<sup>21c</sup>

**Acknowledgment.** Financial support from the Dirección General de Enseñanza Superior (Research grant to C.M.D. and Project PB96-0824) and Junta de Andalucía is gratefully acknowledged. J.A.L. thanks the CONACYT and the University of Guanajuato (Mexico) for a studentship. We also thank the University of Sevilla for the use of its analytical and NMR facilities.

**Supporting Information Available:** Tables of atomic coordinates, thermal parameters, and bond lengths and angles for **4** and **5**. This material is available free of charge via the Internet at <http://pubs.acs.org>.

OM000044G